

# Surface topography and hydrogen sensor response of APCVD grown multilayer graphene thin films

D. Dutta<sup>1,5</sup> · E. Bontempi<sup>2</sup> · Y. You<sup>3,4</sup> · S. Sinha<sup>3,4</sup> · J. Das<sup>5</sup> · S. K. Hazra<sup>6</sup> · C. K. Sarkar<sup>1</sup> · S. Basu<sup>1</sup>

Received: 11 May 2016 / Accepted: 5 August 2016 / Published online: 10 August 2016  
© Springer Science+Business Media New York 2016

**Abstract** Atmospheric pressure chemical vapour deposition was employed to deposit graphene thin films on thermally oxidized p-silicon substrates. Raman spectroscopy and energy dispersive spectroscopy revealed the multilayer nature and the composition of the grown graphene films respectively. The defective nature and the defect density of the graphene films were determined from the Raman experiments. Field effect scanning electron microscopy, transmission electron microscopy and atomic force microscopy were used to study the surface morphology of the multilayer graphene films. The film topography was sensitive to temperature and time of growth. A suitable growth mechanism has been proposed to explain the topographical observations. The large surface area of the multilayer films was found to be suitable for hydrogen sensor applications and the sensing results were correlated with the morphology of the grown films.

## 1 Introduction

Graphene, a single layer or the multilayers of graphite has several advantages for the applications in solar cells, low resistance electrodes, ultra capacitors, sensors and many other important devices due to its extraordinary structural, mechanical and electrical properties [1]. At present, graphene has been considered as a challenging material for innovative research and development and such endeavors will in turn reveal more exciting properties of this material [2, 3]. The ability to synthesize graphene films on various substrates by the methods compatible with the current industrial technology is important for its future applications. The methods so far tried for graphene synthesis are exfoliation [4], chemical synthesis and chemical vapour deposition (CVD) [5–8]. The surface properties of graphene which are important for device applications depend very much on the method of preparation. CVD is an established technique for the large scale production of different important semiconductor materials including graphene. The other methods to develop graphene films are still confined to the laboratory scale. In whatever method the graphene films are synthesized, the imperfections in the grown films limit its applicability to a particular area. APCVD is a simple and effective technique to grow large area graphene films. However, APCVD films have imperfections, which need careful tuning of experimental parameters to achieve large scale uniformity both in micro and macro dimensions [9]. In this investigation APCVD was employed to grow the multilayer graphene films and thoroughly characterized to establish the suitability of the films for gas sensor applications. Normally, thin graphene films are characterized by tools like Raman spectroscopy and atomic force microscopy (AFM) to get various useful information for device applications. Raman spectroscopy is

---

✉ S. Basu  
sukumarbasu@gmail.com

<sup>1</sup> Department of ETCE, IC Design and Fabrication Centre, Jadavpur University, Kolkata, India

<sup>2</sup> Dipartimento di Ingegneria Meccanica e Industriale, Brescia University, Brescia, Italy

<sup>3</sup> Department of Physics, University of New Haven, West Haven, CT, USA

<sup>4</sup> Department of Electrical and Computer Engineering, University of New Haven, West Haven, CT, USA

<sup>5</sup> Department of Physics, Jadavpur University, Kolkata, India

<sup>6</sup> Department of Physics and Materials Science, Jaypee University of Information Technology (JUIT), Warknaghat, Himachal Pradesh, India

the most reliable method to establish the formation and the defect density of the prepared graphene films. AFM is an important tool for getting the idea about the morphology of the thin films. In 2009 Paredes et al. [10] used AFM to characterize the chemically prepared reduced graphene oxide nano sheets. AFM height analysis is reported for thickness measurements of thin graphene films [11–14] with the limitation of the roughness and the non-uniformity of grown films. On the other hand, FESEM study exposes the surface topography of both single layer and multilayer graphene [15]. Moreover, FESEM can also be employed to ascertain the growth pattern (haphazard or unidirectional) along with TEM results. In this study we employed Raman spectroscopy, FESEM, TEM and AFM to characterize the morphology of APCVD grown multilayer graphene film, EDS was carried out to find out the composition of the graphene film. The effect of growth temperature and time on the morphology of APCVD grown MLG has also been discussed. Finally, we have reported a cursory study on the potential use of the MLG films grown by APCVD for hydrogen response.

## 2 Experimental

### 2.1 APCVD growth

The multilayer graphene was deposited on the thermally oxidized p-Si [resistivity (5–10)  $\Omega$  cm and <100> orientation] by atmospheric pressure chemical vapour deposition (APCVD) The clean silicon substrate was first coated with a layer of catalytic Cu film ( $\sim$ 300 nm) by electron-beam evaporation. Before starting the growth run at a particular temperature, the substrate was annealed (at the growth temperature) for 1 h in a reducing atmosphere consisting of a mixture of hydrogen ( $H_2$ ) and nitrogen ( $N_2$ ) by maintaining constant gas flow ratio 25:500 (SCCM). This heat treatment would initiate the grain growth and eliminate imperfections in the copper film, which could help in the uniform nucleation at the Cu/SiO<sub>2</sub> interface. After the annealing treatment the high purity methane ( $CH_4$ ) gas was added to the flow of a mixture of high purity hydrogen and nitrogen with a ratio of  $H_2:CH_4:N_2$ :10:25:300 (SCCM) for the growth of graphene [16].

$CH_4$  molecules dissociate into carbon (C) atoms over the hot catalytic metal (Cu) surface. These carbon atoms diffuse into the Cu/SiO<sub>2</sub> interface, and eventually nucleate on SiO<sub>2</sub> to form the hexagonal graphene network. The above process flow is schematically represented in Fig. 1. Similar growth technique is reported by Su et al. [17].

After the growth was completed the CVD furnace was cooled down to 350 °C at the rate of 5 °C/min and then to the room temperature by switching off the electric power.

The samples were unloaded from the CVD chamber and were treated with 1(M) ferric chloride ( $FeCl_3$ ) mixed with 1(M) hydrochloric acid (HCl) solution for 24 h to remove the Cu layer. After the complete removal of Cu film the samples were carefully rinsed in an ultrasonic bath using deionised water and were dried at room temperature.

Figure 2 demonstrates a temperature gradient from 1000 to 900 °C within the length of 6 cm of the CVD furnace fabricated in our laboratory. We verified experimentally and confirmed that the gradient remains constant without any change of temperature with the specified power supplied to the furnace. Therefore, in a single CVD run we could prepare graphene samples at three different temperatures e.g. 1000, 950 and 900 °C simultaneously. Two sets of graphene samples were prepared by flowing  $CH_4$  gas for 8 and 15 min respectively. We observed that for the deposition time <8 min no significant Raman signatures of the samples were obtained.

### 2.2 Characterizations and sensor study

The Raman spectra of the grown graphene films were collected by using Labram Dilor JY spectrometer, with a 632.8 nm He–Ne laser source. The AFM images were collected from the instrument with model no.: Nano-R2 of Pacific Technology. JEOL JSM-6390 LV instrument was used to collect the FESEM images and EDS data of the multilayer graphene surfaces. For TEM image the model JEM 2100 (JEOL, Japan) was used. A dynamic sensor chamber was employed to evaluate the hydrogen sensor performance of the multilayer graphene by using a planar device fabricated by depositing two Pd electrodes on the lateral surface by e-beam evaporation. The devices were exposed to different concentrations of hydrogen in air in the temperature range 40–150 °C, and the data were recorded by Keithley Pico-ammeter with voltage source (Model 6487, M/S Keithley Instruments).

## 3 Results and discussion

### 3.1 Raman study

The Raman spectroscopy is a useful technique for the confirmation of graphene formation [16, 18]. From Raman spectra the ratio ( $I_{2D}/I_G$ ) and ( $I_D/I_G$ ) are two important components for the determination of the multilayer character and the defects/disorders present in the graphene layers [19]. The Raman spectra for the graphene samples grown at 900, 950, and 1000 °C for 8 min and also for 15 min are shown in Fig. 3. The Raman signatures of our samples confirm the formation of defective graphene film with multilayer character.

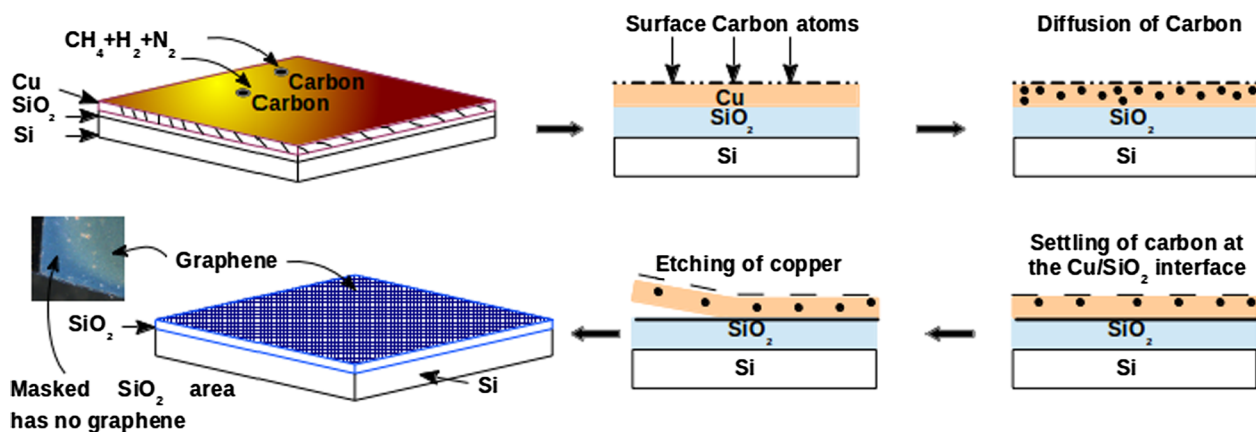


Fig. 1 Schematic representation of the graphene deposition process

Fig. 2 Schematic of the CVD chamber with the substrates loaded at the defined temperature zone

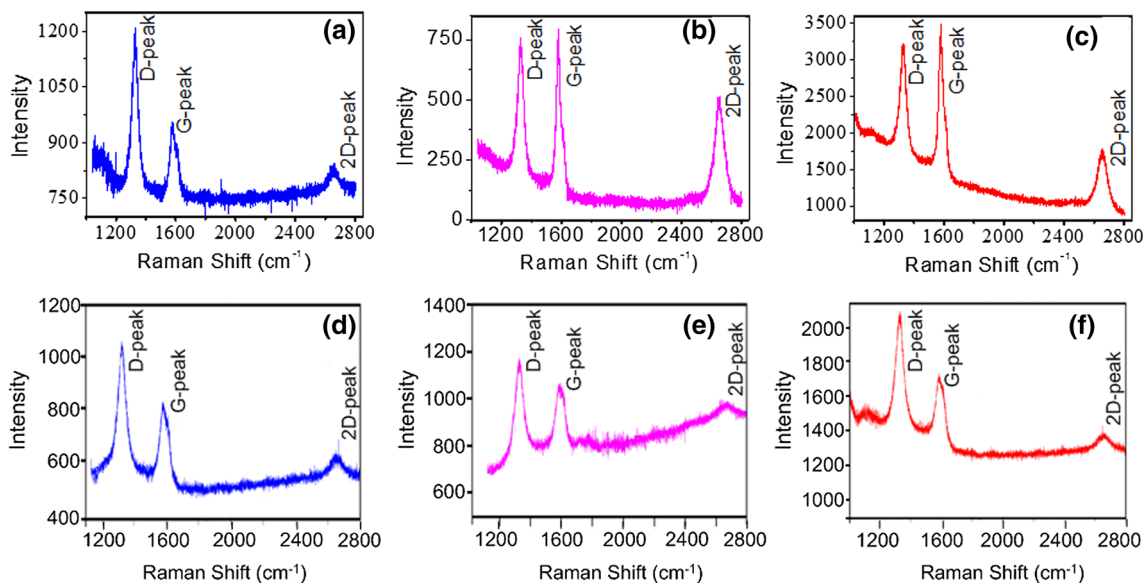
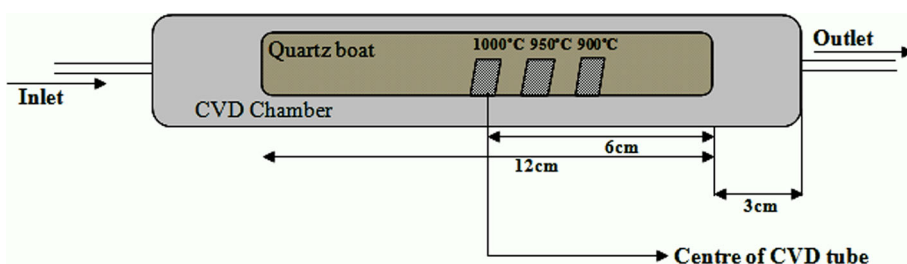
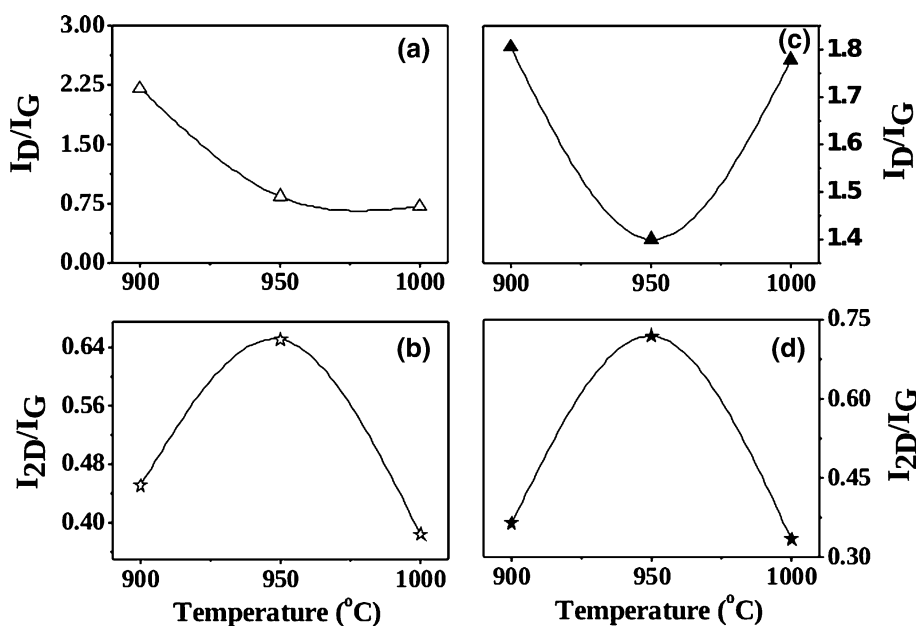


Fig. 3 Raman spectroscopy of APCVD grown graphene films for 8 min at a 900 °C, b 950 °C, c 1000 °C and for 15 min at d 900 °C, e 950 °C, f 1000 °C

The value of  $I_{2D}/I_G$  &  $I_D/I_G$  in each case is calculated and presented in Fig. 4. Normally the  $I_{2D}/I_G$  &  $I_D/I_G$  represent respectively the single/multilayer nature and the defect density of graphene films.  $I_{2D}/I_G$  value is higher when the prepared graphene film approaches toward single layer [20, 21]. It is evident from Fig. 4 that both the multilayer nature and the defect density of the graphene films

vary with the increasing growth temperature. It is observed from Fig. 4a, c that the defect density ( $I_D/I_G$ ) decreases at 950 °C and then increases with the increase of temperature to 1000 °C. Also it is found from Fig. 4b, d that there is increase of  $I_{2D}/I_G$  from 900 to 950 °C and then there is a decreasing trend. Both these observations support the optimum growth temperature of 950 °C for this set of

**Fig. 4** Variation of  $I_D/I_G$  and  $I_{2D}/I_G$  with growth temperature for 8 min (a, b) and for 15 min (c, d)



growth conditions. The decreasing trend of  $I_{2D}/I_G$  with the increase in temperature from 950 to 1000 °C indicates the increase in multilayer character which is probably due to secondary and tertiary nucleation. The secondary/tertiary atomic clusters eventually grow in size at relatively higher temperatures. Basically, some clusters in close proximity can merge at higher temperatures and the others can grow in size. Such complexity in growth process can impart more multilayer character to the graphene films. Also, the decreasing trend of  $I_D/I_G$  ratio with the increase in temperature from 900 to 950 °C indicates that the defects in the grown films are getting thermally annealed at relatively higher temperatures due to migration of atoms/clusters with the available thermal energy to form relatively less defective graphene matrix. However, the increase in defect density at 1000 °C is due to secondary growth as discussed earlier. At low growth temperature the origin of defects could be the lack of granular homogeneity in the catalytic copper layer. Low temperature growth of graphene by CVD has also been reported [22]. Therefore, growth temperature plays a pivotal role in depositing graphene film by APCVD and in tuning the defect density in single/multilayer graphene.

Along with the influence of growth temperature, the multilayer nature and the defect density of the graphene films are also dependent on the growth time. Figure 4 demonstrates that 950 °C is the breaking temperature for both defect density and multilayer nature of the deposited graphene film. We observe that the Raman signature  $I_D/I_G$  (Fig. 4a) representing the defect density reduces with the increase of temperature and shows a trend of saturation for

the growth time of 8 min. But for the growth time of 15 min (Fig. 4c)  $I_D/I_G$  i.e. the defect density increases after 950 °C. This indicates further growth of graphene layer at higher temperature and for longer time. This is further supported by the variation of  $I_{2D}/I_G$ , the Raman signature for the single/multilayer nature (Fig. 4b, d). The multilayer nature reduces as the growth temperature increases from 900 to 950 °C. Again, the multilayer growth enhances as the temperature increases from 950 to 1000 °C due to further growth of the graphene layer. This is supported by the increase and then decrease of  $I_{2D}/I_G$  as the temperature increases from 900 to 1000 °C. With the increase of growth time the enhanced incorporation of carbon atoms occur at the defective sites of the individual graphene layer due to the availability of sufficient number of carbon atoms generated from the decomposition of methane for a longer period.

Raman studies were extended to graphene films deposited for 8-min at three different temperatures and the G-band images were recorded [23]. The Raman images of G-band intensity of the graphene films are shown in Fig. 5.

It is clear from Fig. 5 that the graphene sample grown at 1000 °C shows most intense G-band image with almost uniform surface topography. The intensity of the G-band image is reduced with a relatively rough surface topography for the graphene sample grown at 950 °C. However, at 900 °C there is discontinuity in the topography as it is shown in Fig. 5. Therefore, we can infer from this study that the uniform and smooth surface topography is related to the thicker graphene film deposited by APCVD at higher temperature. The subsequent AFM studies

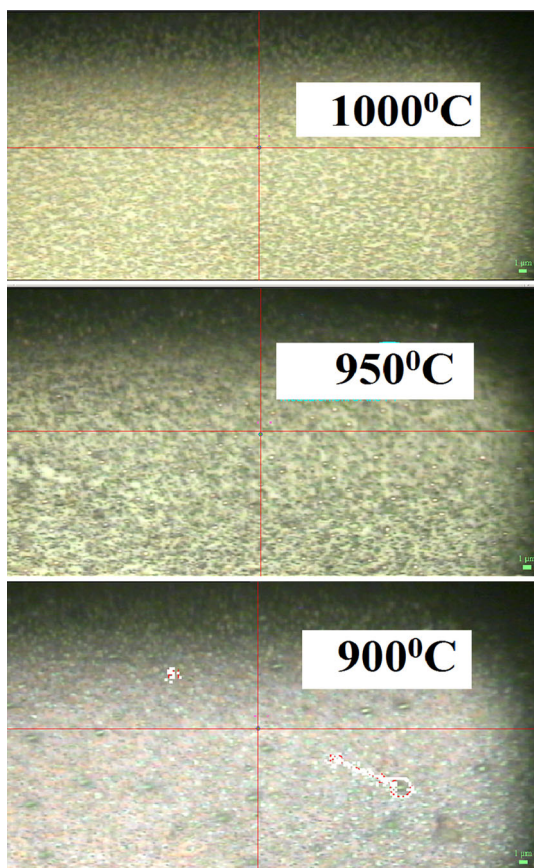


**Fig. 5** Raman image of the graphene samples grown at **a** 900 °C, **b** 950 °C and **c** 1000 °C for 8 min

further confirm the observations obtained from Raman analysis.

### 3.2 FESEM and TEM studies

The nature of continuity and growth at the microscopic domain of the graphene films is further studied with the help of FESEM [24] and TEM. Basically, the visualization of the surface coverage for the minimum growth period is sufficient to understand the growth mechanism. Moreover longer growth time will only increase the surface coverage either uniformly or non-uniformly. The FESEM study of the graphene surfaces grown at 900, 950 and 1000 °C for 15 min has already been reported by us [25]. In this study the surface topography of three graphene samples grown at 900, 950 and 1000 °C for a period of 8 min are presented. The FESEM images of graphene surfaces are shown in Fig. 6. An increase in the coverage of the substrate with somewhat random growth of graphene with the increase of temperature is visible from the FESEM images. While Fig. 6a shows the patch wise formation of graphene film on the substrate at 900 °C, Fig. 6b, c indicate that the films grown at 950 and 1000 °C have relatively more dense

morphology. This is further supported by TEM images. Figure 5 also shows that the surface of the graphene film grown at 1000 °C is more uniform than the films grown at 900 and 950 °C. Stringent optimization of the growth process is necessary to obtain electronic grade graphene films. On the other hand, defective surface morphology is an advantage for certain type of applications like gas sensors because the defects increase the active gas adsorption sites keeping the geometrical device area constant and improves the gas sensing performance. FESEM and TEM studies were performed to clarify the growth morphology in the temperature range 900–1000 °C. While the FESEM pictures (Fig. 6a–c) solicit for more fibrous growth with the increase of temperature covering the larger area of the substrate TEM images confirm the finger like growth of graphene at different directions as shown in Fig. 6d–f. HRTEM (High Resolution Transmission Electron Microscope) could better resolve the observed growth but this study could not be extended due to unavailability of this sophisticated experimental facility. Nevertheless, a random growth of graphene has been strongly indicated by TEM.

### 3.3 Energy dispersive X-ray spectroscopy (EDS)

The energy dispersive X-ray spectroscopy (EDS) was used to find out the elements present in the CVD grown graphene samples and to establish the purity of the films. A single sample was chosen for this study and a simple line scan was performed. A typical spectrum obtained from the sample grown at 900 °C for 8 min is shown in Fig. 7. Table 1 shows the percentage of C, Si and O in the graphene sample. The peaks for Si and O appear from SiO<sub>2</sub>/Si substrate, while the peak for C indicates the presence of graphene on the substrate.

### 3.4 AFM studies

AFM (Atomic Force Microscopy) is a reliable tool [4, 26] for the morphological characterization of graphene thin film due to its high spatial resolution and different modes of operation. The AFM imaging was performed to understand the quality of the APCVD grown graphene thin film on SiO<sub>2</sub>/Si substrate. The AFM images of the graphene samples grown at three different temperatures and for two different time periods are shown in Fig. 8. The AFM image of the bare substrate (without graphene) is shown separately in Fig. 9a.

Figure 8 shows that graphene surfaces grown for longer period (15 min) have relatively more compact morphology. Both the individual clusters and the inter-cluster gap are reduced with the increase in growth time. The surface roughness values for the bare substrate (~53.7 nm) and the graphene layer on the substrate are obtained from the

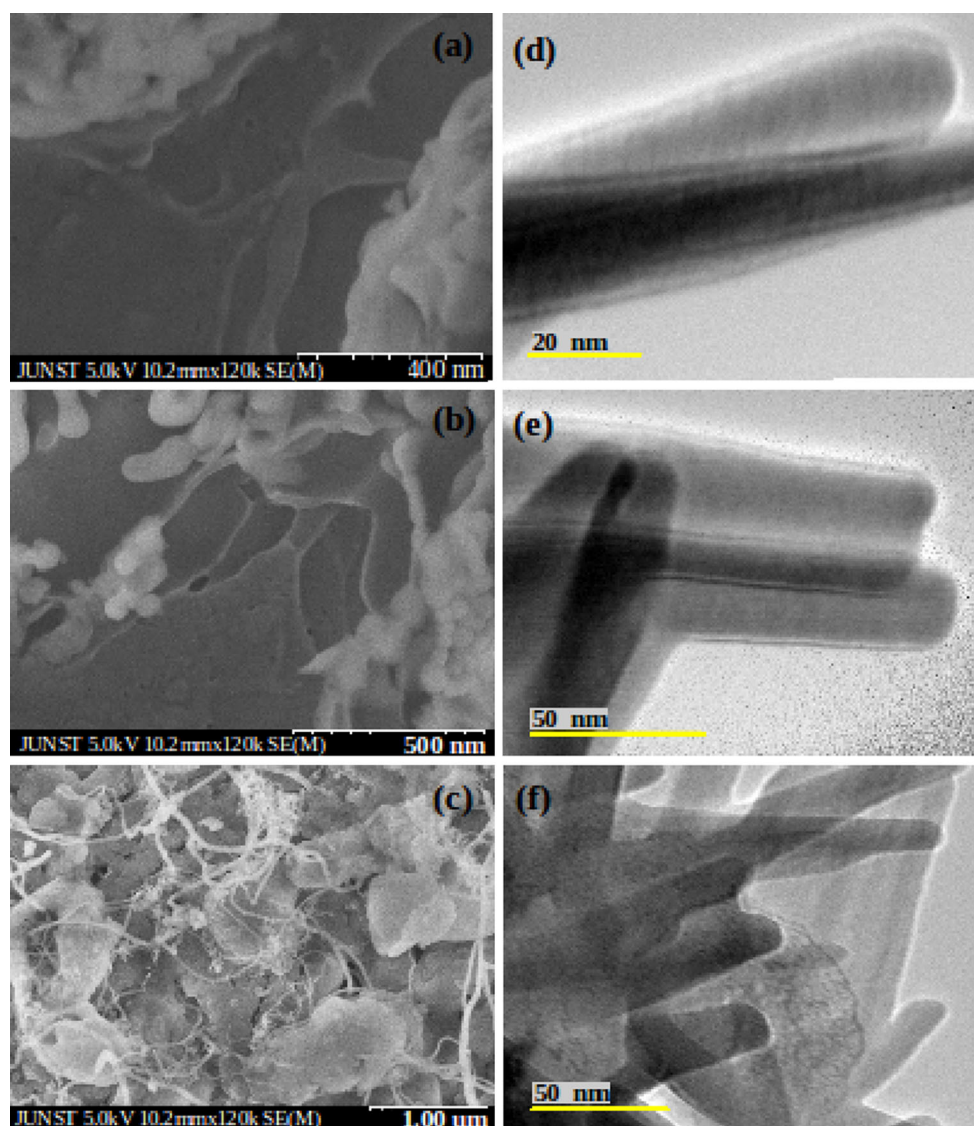


**Fig. 6** FESEM (a–c) and TEM (d–f) images of the graphene films grown at 900, 950, and 1000 °C for 8 min respectively

AFM studies. The variation of roughness of graphene films with growth temperature and time is presented in Fig. 9b. It is observed that with the increase in growth temperature and growth time, the surface roughness decreases. This is due to the fact that the individual carbon islands merge and make the surface more smooth for the growth at higher temperature and for longer time. As a result the surface roughness of the grown graphene film reduces. It is further evident from Fig. 9b that the graphene sample deposited for 8 min is rougher than that deposited for 15 min for any temperature in the range 900–1000 °C. But the slope of the curve for 15 min deposition becomes almost horizontal and parallel to temperature axis at higher temperature thereby showing a trend of saturation. Thus it indicates that even by further increase of deposition time the surface quality of graphene layer may not improve.

### 3.5 Proposed growth mechanism

On the basis of the above discussions on the topography a simple growth mechanism of graphene films obtained by APCVD is proposed in Fig. 10.

The growth proceeds via heterogeneous nucleation. The individual carbon atoms percolate down the copper film and start the nucleation at the Cu/SiO<sub>2</sub> interface. The initial interface coverage is governed by the smoothness of the substrate, and from Fig. 9a, it is apparent that the SiO<sub>2</sub> layer on the substrate is almost smooth. However, there are undulation or rough projections on the SiO<sub>2</sub> layer (as revealed by AFM) (Fig. 9a). Hence during the formation of the first graphene monolayer, secondary and tertiary nucleation eventually start at the rough substrate imperfections. Likewise, before the completion of the second

**Fig. 7** EDS of a graphene sample deposited at 900 °C for 8 min

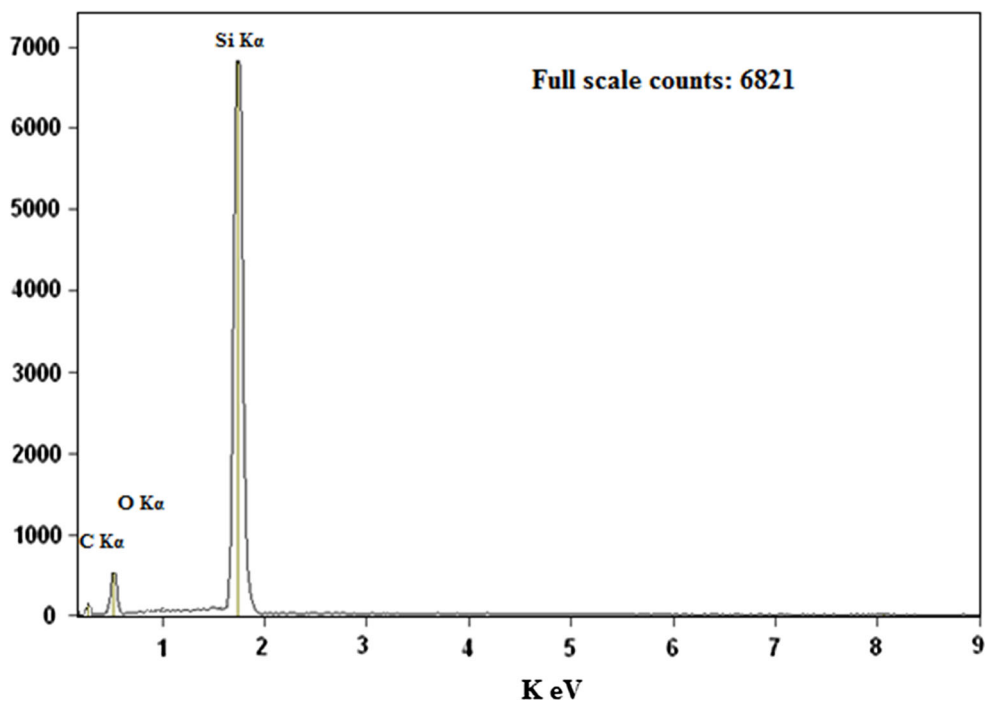


**Table 1** Percentage of the elements present in a graphene film

Elements line	Wt%	At%	Formula
C K	3.85	7.48	C
O K	20.08	29.30	O
Si K	76.07	63.23	Si
Total	100.00	100.00	

monolayer the third layer can start growing and similarly the fourth layer can start before the second or third layer growth is complete. Therefore, at the defective locations, multiple layers can start growing in random directions. As a matter of fact, such versatile growth options in this heterogeneous growth process can lead to the development of islands like graphene clusters, prominently seen in the AFM images (Fig. 8). If higher temperature and suitable growth time are provided the islands can join with each other and make the surface uniform and smooth. This is in agreement with our experimental observation (Fig. 9b) that the roughness of the graphene film reduces with the increase in growth time and temperature.

### 3.6 Evaluation of the graphene morphology via hydrogen sensing

The graphene samples grown at 1000 °C for 8 min and for 15 min were chosen for the hydrogen sensor study. Simple planar device with Pd/graphene/Pd junctions was fabricated with the grown graphene films by depositing two

palladium contacts on the surface of the films by e-beam evaporation for the sensor studies. Normally high surface area materials have large number of active sites, which can ensure higher gas adsorption at relatively lower temperature. The morphological studies have revealed that the grown nanostructured graphene films are defective and have high surface roughness favourable for hydrogen sensing and hydrogen storage applications. The variation of the morphology and especially the reduction in defect density of the grown films with the increase in growth time are evident from AFM and Raman studies. Therefore, it is likely that such morphology will influence the gas adsorption traits of these films. The device with 8-min grown graphene film was responsive to hydrogen at relatively lower temperature ( $\sim 50$  °C) while the device with 15-min grown graphene film was sensitive to hydrogen above 100 °C. Table 2 presents the comparative sensing results. The detailed sensor studies with similarly grown samples have been reported [25, 27]. The difference in temperature of sensing is directly related to the difference in morphology of the films. It is expected that the compact and less defective morphology obtained with high temperature and longer growth time, requires high activation energy for adsorbing hydrogen, and therefore the devices based on these films are giving appreciable gas response only at elevated temperatures. Also, response magnitude (which directly indicates the gas adsorption ability of the junctions) reduces with the increase in growth time, thereby re-establishing the compact and relatively less defective nature of the 15 min grown films. But the surface

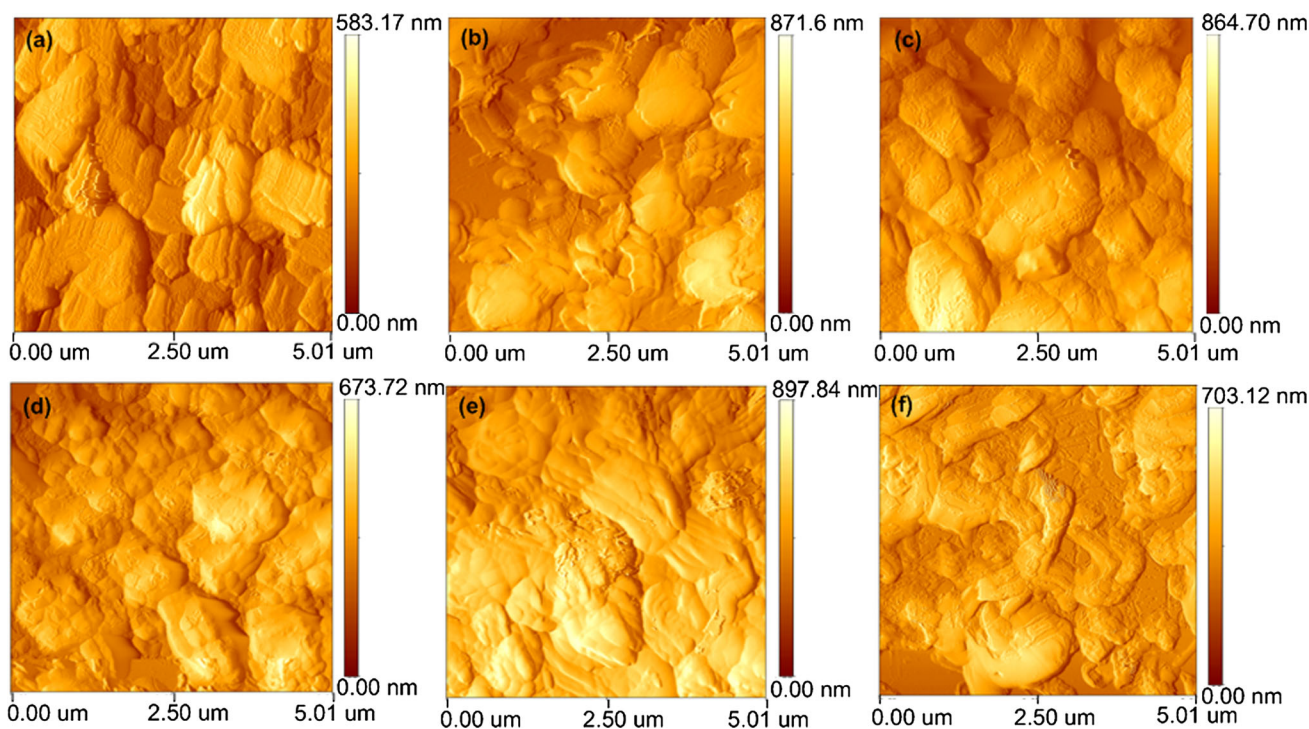


**Fig. 8** AFM images of the graphene films grown for 8 min at **a** 900 °C, **b** 950 °C and **c** 1000 °C and AFM images of the graphene films grown for 15 min at **d** 900 °C, **e** 950 °C and **f** 1000 °C

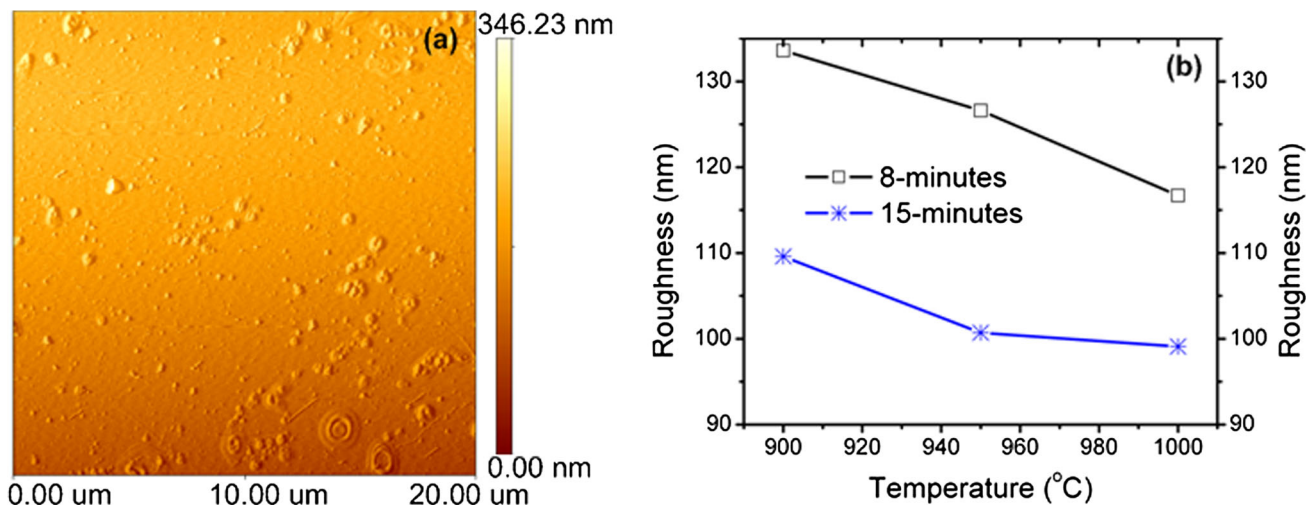


**Fig. 9** **a** AFM image of the bare SiO<sub>2</sub>/Si substrate which was used for growth of graphene film. **b** Variation of the roughness of the grown graphene films on SiO<sub>2</sub>/Si substrate with time and temperature of deposition

grown for relatively shorter time has much lower temperature of adsorption ( $\sim 50$  °C), due to high surface activity of the defective morphology. Moreover, it is also observed that the recovery is delayed at low sensing temperature due to the longer desorption time from the films with defective morphology. However, the rough and defective morphology have been employed to develop the graphene based heterojunction sensor [28] where titanium dioxide plays a crucial role in the faster charge transport at the junction. So

it can be inferred that the performance of the hydrogen sensors based on the APCVD grown graphene films can be improved further with the refinement of the growth parameters.

The hydrogen sensing result shown in Table 2 clearly indicates higher response by the graphene sample deposited for 8 min. But the response time and recovery time are much shorter for the sample deposited for 15 min. In our earlier discussion we have indicated much higher surface

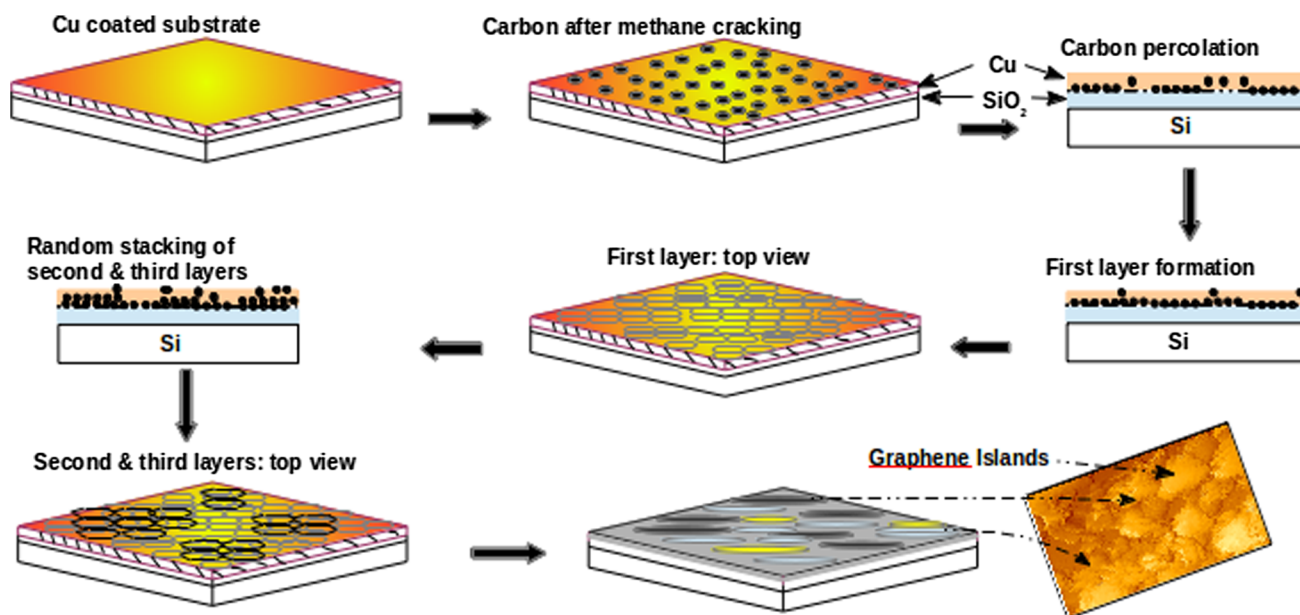


**Fig. 10** Growth model of graphene film deposited by APCVD

**Table 2** Comparison of hydrogen response results of APCVD grown graphene thin films with two different growth times

Material	Growth time (Min)	Sensing temperature (°C)	Response time (s)	Recovery time (s)	%Response
Graphene	8	50	~ 19	~ 612	~ 69
Graphene	15	110	~ 12	~ 29	~ 6

roughness of the samples deposited for 8 min compared to that deposited for 15 min (Fig. 9b). This is further supported by the higher response of ~69 % of the samples deposited for 8 min due to higher hydrogen adsorption. On the other hand, the faster response and faster recovery by the sample deposited for 15 min are due to smoother surface, faster charge transfer and quicker desorption.

#### 4 Conclusion

We conclude from our experimental observations that the graphene films are very much susceptible to the CVD growth conditions. It is once again verified that the morphology, multilayer nature and defect density of the deposited graphene films depend very much on the temperature and time of APCVD growth. The films obtained by 8-min growth are quite rough, which ensures high surface area for hydrogen adsorption and sensor response. But the roughness decreases with the increase in the growth temperature. Growth at higher temperature reduces the defect density of the films and produces a smooth surface. This is verified from the hydrogen sensor studies. The variation in morphology affects the gas adsorption

characteristics, including the temperature of adsorption. For electronic applications more stringent growth optimization is necessary to reduce the defect density and the multilayer nature and to improve the quality of the APCVD grown graphene films.

**Acknowledgments** D. Dutta thankfully acknowledges CSIR, Government of India for providing the junior research fellowship to carry out the work. S.K. Hazra is thankful to IC Design and Fabrication Centre, Department of ETCE, Jadavpur University, India for providing the collaborative research opportunity. The authors gratefully acknowledge the help of Prof. S. Basumajumdar, Materials Science Centre, IIT Kharagpur, India for TEM images.

#### References

1. S. Basu, P. Bhattacharyya, Recent developments on graphene and graphene oxide based solid state gas sensors. *Sens. Actuators B* **173**, 1–21 (2012)
2. S.K. Hazra, S. Basu, Chemical modification of graphene and applications for chemical sensors, in *Chemical Functionalization of Carbon Nanomaterials-Chemistry and Applications*, ed. by V.K. Thakur, M.K. Thakur (CRC Press, Taylor and Francis, Boca Raton, 2015), pp. 914–937
3. M. Miculescu, V.K. Thakur, F. Miculescu, S.L. Voicu, Graphene-based polymer nanocomposite membranes: a review. *Polym. Adv. Technol.* **27**(7), 844–859 (2016)

4. Y.M. Chang, H. Kim, J.H. Lee, Y.W. Song, Multilayered graphene efficiently formed by mechanical exfoliation for nonlinear saturable absorbers in fiber mode-locked lasers. *Appl. Phys. Lett.* **97**, 211102 (2010)
5. A.N. Obraztsov, E.A. Obraztsova, A.V. Tyurnina, A.A. Zolotukhin, Chemical vapor deposition of thin graphite films of nanometer thickness. *Carbon* **45**, 2017–2021 (2007)
6. Q. Yu, J. Lian, S. Siriponglert, H. Li, Y.P. Chen, S.S. Pei, Graphene segregated on Ni surfaces and transferred to insulators. *Appl. Phys. Lett.* **93**, 113103 (2008)
7. K.S. Kim, Y. Zhao, H. Jang, S.Y. Lee, J.M. Kim, K.S. Kim, J.H. Ahn, P. Kim, J.Y. Choi, B.H. Hong, Large-scale pattern growth of graphene films for stretchable transparent electrodes. *Nature* **457**, 706–710 (2009)
8. A. Reina, X. Jia, J. Ho, D. Nezich, H. Son, V. Bulovic, M.S. Dresselhaus, J. Kong, Large area, few-layer graphene films on arbitrary substrates by chemical vapor deposition. *Nano Lett.* **9**(1), 30–35 (2009)
9. L.P. Ma, W.C. Ren, Z.L. Dong, L.Q. Liu, H.M. Cheng, *Chin. Sci. Bull.* **57**(23), 2995–2999 (2012). doi:10.1007/s11434-012-5335-4
10. J.I. Paredes, S.V. Rodil, P.S. Fernandez, A.M. Alonso, J.M.D. Tascon, Atomic force and scanning tunnelling microscopy imaging of graphene nanosheets derived from graphite oxide. *Langmuir* **25**(10), 5957–5968 (2009)
11. K.H. Liao, A. Mittal, S. Bose, C. Leighton, K.A. Mkhoyan, C.W. Macosko, Aqueous only route toward graphene from graphite oxide. *ACS Nano* **5**, 1253–1258 (2011)
12. Y. Zhu, M.D. Stoller, W. Cai, A. Velamakanni, R.D. Piner, D. Chen, R.S. Ruoff, Exfoliation of graphite oxide in propylene carbonate and thermal reduction of the resulting graphene oxide platelets. *ACS Nano* **4**(2), 1227–1233 (2010)
13. F. Hauquier, D. Alamarguy, P. Viel, S. Noël, A. Filoramo, V. Hucd, F. Houz a, S. Palacin, Conductive-probe AFM characterization of graphene sheets bonded to gold surfaces. *Appl. Surf. Sci.* **258**, 2920–2926 (2012)
14. O. Albrektsen, R.L. Eriksen, S.M. Novikov, D. Schall, M. Karl, S.I. Bozhevolnyi, A.C. Simonsen, High resolution imaging of few-layer graphene. *J. Appl. Phys.* **111**, 064305 (2012)
15. H. Hiura, H. Miyazaki, K. Tsukagoshi, Determination of the number of graphene layers: discrete distribution of the secondary electron intensity stemming from individual graphene layers. *Appl. Phys. Express* **3**, 095101 (2010). (**The Japan Society of Applied Physics**)
16. D. Dutta, A. Hazra, J. Das, S.K. Hazra, V.N. Lakshmi, S.K. Sinha, A. Gianonchelli, C.K. Sarkar, S. Basu, Growth of multilayer graphene by chemical vapor deposition (CVD) and characterizations. *J. Nanomater. Mol. Nanotechnol.* **3**(5), 004 (2014). doi:10.4172/2324-8777.S1-004
17. C.-Y. Su, A.-Y. Lu, C.-Y. Wu, Y.-T. Li, K.-K. Liu, W. Zhang, S.-Y. Lin, Z.-Y. Juang, Y.-L. Zhong, F.-R. Chen, L.-J. Li, Direct formation of wafer scale graphene thin layers on insulating substrates by chemical vapor deposition. *Nano Lett.* **11**, 3612–3616 (2011). doi:10.1021/nl201362n
18. W. Liu, H. Li, C. Xu, Y. Khatami, K. Banerjee, Synthesis of high-quality monolayer and bilayer graphene on copper using chemical vapor deposition. *Carbon* **49**, 4122–4130 (2011)
19. A. Das, B. Chakraborty, A.K. Sood, Raman spectroscopy of graphene on different substrates and influence of defects. *Bull. Mater. Sci.* **31**, 579–584 (2008)
20. Q. Huang, D. Zeng, S. Tian, C. Xie, Synthesis of defect graphene and its application for room temperature humidity sensing. *Mater. Lett.* **83**, 76–79 (2012)
21. A.-Y. Lu, S.-Y. Wei, C.-Y. Wu, Y. Hernandez, T.-Y. Chen, T.-H. Liu, C.-W. Pao, F.-R. Chen, L.-J. Li, Z.-Y. Juang, Decoupling of CVD graphene by controlled oxidation of recrystallized Cu. *RSC Adv.* **2**, 3008–3013 (2012)
22. Z. Li, P. Wu, C. Wang, X. Fan, W. Zhang, X. Zhai, C. Zeng, Z. Li, J. Yang, J. Hou, Low-temperature growth of graphene by chemical vapor deposition using solid and liquid carbon sources. *ACS Nano* **5**(4), 3385–3390 (2011). doi:10.1021/nn200854p
23. Z. Ni, Y. Wang, T. Yu, Z. Shen, Raman spectroscopy and imaging of graphene. *Nano Res* **1**, 273–291 (2008)
24. H. Zhang, P.X. Feng, Fabrication and characterization of few-layer graphene. *Carbon* **48**, 359–364 (2010)
25. D. Dutta, A. Hazra, S.K. Hazra, J. Das, S. Bhattacharyya, C.K. Sarkar, S. Basu, Performance of a CVD grown graphene based planar device for hydrogen gas sensor. *Meas. Sci. Technol.* **26**, 115104 (2015)
26. Y. You, V.N. Lakshmi, S.K. Sinha, D. Dutta, C.K. Sarkar, S. Basu, AFM Characterization of Multilayered Graphene Film Used as Hydrogen Sensor. in *ASEE 2014 Zone I Conference*, University of Bridgeport, Bridgeport, 2014
27. D. Dutta, S.K. Hazra, J. Das, C.K. Sarkar, S. Basu, Temperature- and hydrogen-gas-dependent reversible inversion of n/p- type conductivity in CVD-grown multilayer graphene (MLG) film. *J. Electron. Mater.* **45**(6), 2861–2869 (2016). doi:10.1007/s11664-016-4381-0
28. D. Dutta, S.K. Hazra, J. Das, C. Sarkar, S. Basu, Studies on p-TiO<sub>2</sub>/n-graphene heterojunction for hydrogen detection. *Sens. Actuators B* **212**, 84–92 (2015)